



A combined experimental and TD-DFT investigation of three disperse azo dyes having the nitroterephthalate skeleton



Mininath S. Deshmukh, Nagaiyan Sekar*

Tinctorial Chemistry Group, Department of Dyestuff Technology, Institute of Chemical Technology, Nathalal Parekh Marg, Matunga, Mumbai, Maharashtra 400 019, India

ARTICLE INFO

Article history:

Received 6 July 2013
Received in revised form
23 October 2013
Accepted 25 October 2013
Available online 10 November 2013

Keywords:

Nitroterephthalate azo dyes
Photo-physical properties
Light fastness
TD-DFT
Solvatochromism
Dyeing

ABSTRACT

Three disperse azo dyes were synthesized using diazotized dimethyl 2-amino-5-nitroterephthalate (**5**) followed by the diazo coupling with different N-substituted aromatic amines. The structures of the dyes were confirmed using FT-IR, ¹H NMR, ¹³C NMR, MS and HRMS spectral analysis. The geometries of the azo and hydrazone tautomeric forms of the dyes were optimized at B3LYP/6-31G(d) level of theory, and their electronic excitation properties were evaluated using density functional theory. The computed absorption spectral data of the azo derivatives are in good agreement with the experiment, thus allowing an assignment of the UV–vis spectra. The dyes displayed a broad absorption maximum in the visible region between 498 and 561 nm. The synthesized azo disperse dyes were applied on polyester and nylon fiber and they show very good light fastness and washing fastness properties.

© 2013 Elsevier Ltd. All rights reserved.

1. Introduction

Azobenzenes have versatile applicability ranging from textile dyeing [1], leather dyeing [2], coloring of plastics and polymer [3] to advanced applications such as liquid crystal displays [4], biological and medical studies [5]. In addition to the above features, azobenzenes have interesting properties like the reversible *cis-trans* photoisomerization about the azo π -bond when heated or irradiated in UV [6]. Also, they contribute to the greatest production volume of the dyestuff industry due to simplistic mode of their synthesis with a high atom economy.

The compounds having an intramolecular charge transfer properties are usually functionalized by electron-donating (D) and electron-accepting (A) groups through an azo π -conjugated bridge which makes it possible to reduce the gap between HOMO and LUMO of the molecule for broadening the range of absorption and to study the relationship between the variation of donor/acceptor chromophores and their corresponding photophysical and electrochemical properties [7]. The electron-rich *N,N*-diethylaniline unit is one of the promising donor moiety of donor–acceptor type of functional molecules because of its good electron-donating properties. The presence of acetamido groups at ortho position

relative to the azo bridge is attributed to the hydrogen bonding with azo groups [8]. Also, acetamido and ester moieties are helpful to increase their light fastness, color strength and bright hue as well as photostability properties [9,10].

In this paper, we report synthesis of disperse azo dyes by using traditional azo coupling between *N,N*-diethyl substituted aniline as a coupler and diazonium salt dimethyl 2-amino-5-nitroterephthalate [11]. Density functional theory computations [B3LYP/6-31G(d)] were used to study the geometrical and electronic properties of the synthesized molecules. The solvent effect on absorbance characteristics of the synthesized azo dispersed dyes were studied in solvents of different polarities.

2. Experimental section

2.1. Materials and equipments

Dimethyl 2-aminoterephthalate, *N,N*-diethylaniline, *N*-(3-(diethylamino)phenyl) acetamide, *N*-(3-(diethylamino)-4-methoxyphenyl) acetamide, sodium hydroxide, metamol (dispersing agent) and conc. H₂SO₄ were purchased from s.d. fine chemicals Ltd, Mumbai, India. Solid reagents were characterized by melting point and used without further purification. Liquid reagents distilled at their boiling points and used thereafter. Solvents were used after distillation at their boiling point and drying according to standard processes.

* Corresponding author. Tel.: +91 22 3361 1111/2222/2707 (direct); fax: +91 22 3361 1020.

E-mail addresses: n.sekar@ictmumbai.edu.in, nethi.sekar@gmail.com (N. Sekar).

All the reactions were monitored on precoated silica gel aluminum based plates kisel gel 60 F₂₅₄ Merck, India. Purification of all the compounds was achieved by recrystallization. Melting points were recorded on instrument from Sunder Industrial Product Mumbai by using open capillary and are uncorrected. The absorption spectra of the compounds were recorded on a Spectronic Genesys 2 UV–visible spectrophotometer. The FT-IR spectra were recorded on a Jasco 4100 Fourier Transform IR instrument (ATR accessories). ¹H NMR spectra were recorded on a Varian Cary Eclipse Australia, USA instrument using TMS as an internal standard. Mass spectra were recorded on Finnigan Mass spectrometer. The chemical shift values are expressed in δ ppm using CDCl₃ as a solvent and TMS as an internal standard. DFT calculations were performed on a HP workstation XW 8600 with Xeon processor, 4 GB RAM and Windows Vista as operating system. The software package used was Gaussian 09W. The ground state geometry was optimized at B3LYP level of theory and 6-31G (d) as basis set.

2.2. Computational methods

Gaussian 09 program package was used to optimize geometry and to study the synthesized azo dyes in their azo and hydrazone tautomeric forms [12]. Ground state (S₀) geometry of the dyes in gas and solvent was optimized in their C₁ symmetry using DFT [13]. The Becke's three parameter exchange functional (B3) [14] combining with nonlocal correlation functional by Lee, Yang and Parr (LYP) [15] and basis set 6-31G (d) was used for all atom. Same method was used for vibrational analysis to verify that the optimized structures correspond to local minima on the energy surface. Time Dependent Density Functional Theory (TD-DFT) computations were used to obtain the vertical excitation energies and oscillator strengths at the optimized ground state equilibrium geometries at the same hybrid functional and basis set [16]. All the computations in solvents of different polarities

were carried out using the Self-Consistent Reaction Field (SCRF) under the Polarizable Continuum Model (PCM) [17].

2.3. Synthesis and characterization

The synthetic scheme for the preparation of dyes **7a–7c** is shown in Scheme 1. Dimethyl 2-amino-5-nitroterephthalate (**5**) was prepared by the reported procedure [18] from dimethyl 2-aminoterephthalate (**1**).

2.3.1. Preparation of azo dyes (7a–7c)

2.3.1.1. Preparation of diazotization salt (6). A solution of dimethyl 2-amino-5-nitroterephthalate **5** (2.5 g, 0.01 mol) in concentrated sulfuric acid (10 ml) was slowly added to 1.56 M nitrosylsulfuric acid at 0–5 °C within 1 h. Diazotization reaction was monitored using starch iodide paper. 0.02 g of urea was added to consume excess of nitrous acid. The resulting diazonium solution **6** was further used immediately for coupling.

2.3.1.2. General procedure for coupling. The coupler **a–c** (0.01 mol) were dissolved in 150 ml ethanol at 0–5 °C. Diazonium solution was added dropwise to coupler at 0–5 °C and 5–6 pH adjusted by using 10% sodium hydroxide cold solution. The reaction mixture was further stirred overnight and monitor by using H-acid and starch iodide paper. Precipitated product was filtered and washed with water, crystallized from ethanol to give dyes **7a–7c** respectively.

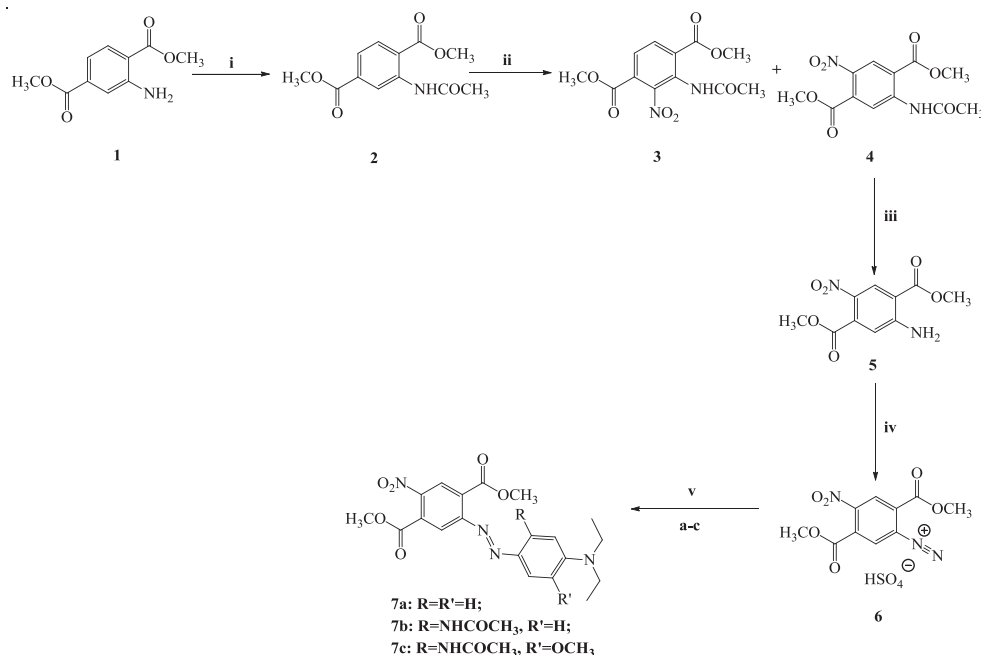
(*E*)-Dimethyl 2-((4-(diethylamino)phenyl)diazenyl)-5-nitroterephthalate (**7a**)

Yield: 72%, **Melting Point:** 40–42 °C.

FAB-MS, m/z: 415.67 [M + H]⁺.

HRMS (FAB+) m/z: calcd for [M + H]⁺, 415.1618; found, 415.1617.

¹H NMR (CDCl₃, 600 MHz): 8.26 (s, 1H, Ar–H), 7.99 (s, 1H, Ar–H), 7.86 (d, 2H, Ar–H, J = 9 Hz), 6.74 (d, 2H, Ar–H, J = 9 Hz),



Reaction condition: (i) Acetic anhydride, Toluene, 80 °C. (ii) Concentrated H₂SO₄, Fuming HNO₃, 0–5 °C.

(iii) Concentrated H₂SO₄, Methanol, 80 °C, 2hr. (iv) Nitrosylsulfuric acid, 0–5 °C.

(v) Ethanol, pH 5–6, 0–5 °C to room temperature.

Scheme 1. Synthesis of azo disperse dyes **7a**, **7b** and **7c**.

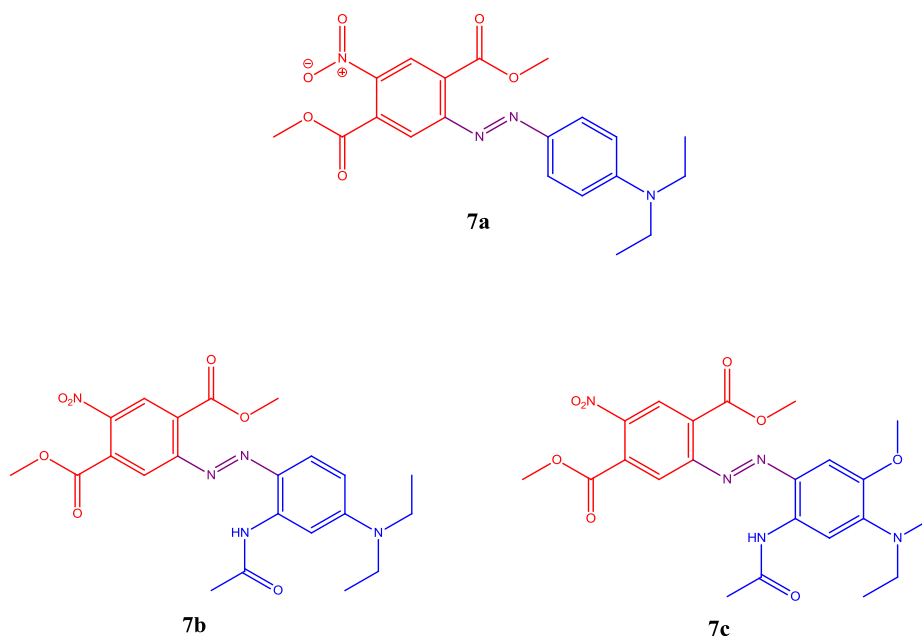


Fig. 1. Structures of the dyes **7a**, **7b** and **7c**.

3.96 (s, 3H, $-\text{OCH}_3$), 3.95 (s, 3H, $-\text{OCH}_3$), 3.47 (q, 4H, $-\text{NCH}_2$), 1.25 (t, 6H, $-\text{CH}_3$).

^{13}C NMR (CDCl_3 , 600 MHz): 12.91(s), 39.47(s), 40.47(s), 44.88, 53.55, 112.05, 118.62, 125.48, 127.62, 129.72, 136.34, 143.08, 146.40, 147.47, 152.66, 165.26, 166.57.

FT-IR: 1254, 1526, 1723, 1593 cm^{-1}

(*E*)-Dimethyl 2-((2-acetamido-4-(diethylamino)phenyl)diazenyl)-5-nitroterephthalate (**7b**)

Yield: 78%, Melting Point: 118–120 °C.

FAB-MS, m/z : 472.20 $[\text{M} + \text{H}]^+$,

HRMS (FAB+) m/z : calcd for $[\text{M} + \text{H}]^+$, 472.1832; found, 472.1832.

^1H NMR (CDCl_3 , 400 MHz): 12.22 (s, 1H, NH), 8.33 (s, 1H, Ar-H), 8.27 (s, 1H, Ar-H), 8.10 (s, 1H, Ar-H), 7.71 (d, 1H, Ar-H, $J = 9.2$ Hz), 6.55 (d, 1H, Ar-H, $J = 8.8$ Hz), 3.95 (s, 6H, $-\text{OCH}_3$), 3.50 (q, 4H, $-\text{NCH}_2$), 2.29 (s, 3H, $-\text{CH}_3$), 1.28 (t, 6H, $-\text{CH}_3$).

^{13}C NMR (CDCl_3 , 600 MHz): 13.01(s), 25.33, 39.47(s), 40.47(s), 44.35, 53.49, 100.96, 109.06, 118.71, 125.83, 127.88, 132.25, 137.08, 146.26, 146.75, 154.00, 165.04, 167.05, 170.16.

FT-IR: 1251, 1522, 1713, 1590, 2968 cm^{-1}

(*E*)-Dimethyl 2-((2-(2-acetamido-4-(diethylamino)-5-methoxyphenyl)diazenyl)-5-nitroterephthalate (**7c**)

Yield: 74%, Melting Point: 133–135 °C.

FAB-MS, m/z : 502.60 $[\text{M} + \text{H}]^+$,

HRMS (FAB+) m/z : calcd for $[\text{M} - \text{H}]^-$ and $[\text{M} + \text{H}]^+$ 500.1781 and 502.1938; found 500.1782 and 502.1938 respectively.

^1H NMR (CDCl_3 , 600 MHz): 8.07 (s, 1H, Ar-H), 7.68 (s, 1H, Ar-H), 7.64 (s, 1H, Ar-H), 6.73 (s, 1H, Ar-H), 4.07 (m, 11H), 2.35 (s, 3H, $-\text{CH}_3$), 1.38 (s, 6H, $-\text{CH}_3$).

^{13}C NMR (CDCl_3 , 600 MHz): 13.50(s), 25.06, 39.64(s), 40.31(s), 46.99, 53.68, 54.07, 100.96, 106.27, 121.22, 127.71, 128.40, 133.15, 137.05, 146.51, 146.90, 148.24, 164.76, 167.87, 169.45.

FT-IR: 1240, 1251, 1522, 1713, 1590, 2968 cm^{-1} .

2.4. Synthetic strategy

Three D- π -A chromophoric dyes have been synthesized by conventional methods. The dyes contain an electron donor *N,N*-diethylaniline group, electron acceptor nitro and carbmethoxy

groups an azo conjugated π -bridge. They were synthesized by azo coupling reaction [11]. The diazotisation was carried out using nitrosylsulfuric acid because of its high reactivity which helps for protonation of the *N*-atom [19]. The resulting diazonium solution **6** were further coupled with the different *N,N*-diethyl substituted aniline (**a–c**) to give the target azo disperse dyes (**7a–7c**) Fig. 1. In the first step, acylation of **1** in acetic anhydride in toluene to give **2**, which on further nitration in fuming HNO_3 and H_2SO_4 gives intermediates **3** (8%) and **4** (92%). The deacylation of **4** in concentrated sulfuric acid and methanol gives **5** (Scheme 1).

The structure of the compounds was confirmed by FTIR, ^1H NMR, ^{13}C NMR, FAB-MS and HRMS spectral analysis. The ^1H NMR spectra of compound **7c** amide $-\text{NH}$ proton exchange with solvent and their HRMS in positive $[\text{M} + \text{H}]^+$ and negative $[\text{M} - \text{H}]^-$ mode was found to be at 502.1938 and 500.1782 respectively, while compound **7a** and **7b** FAB-MS $[\text{M} + \text{H}]^+$ and HRMS $[\text{M} + \text{H}]^+$ is in good agreement with the molecular weight of the compounds.

3. Result and discussion

The absorption properties of the newly synthesized ester containing mono azo disperse dyes are correlated with an analogous reported dye in DMF. The synthesized nitro substituted terephthalate mono azo disperse dyes **7a–7c** are red shifted compared to the reported dyes devoid of nitro group **8a–8c** (Fig. 2) because of the strong electron withdrawing effect of the nitro para to the azo group [20]. The dye **7a–7c** have blue shifted absorption as compared to the reported dye **8d** [21] which may be attributed to the strong electron withdrawing effects of acetonitrile ester (Fig. 2).

3.1. Photo-physical properties

The UV-Vis absorption spectra of 1×10^{-6} mol L^{-1} solution of dyes **7a–7c** were measured in solvent of different polarity, dielectric constant, refractive indices in (Tables 1–3). These newly synthesized terephthalate azo derivatives with D- π -A system consist of an electron-donating *N,N*-diethylaniline unit and electron-withdrawing nitro or carbmethoxy groups conjugated through azo π -bonding exhibited strong red-shifted absorption (Fig. 3). The

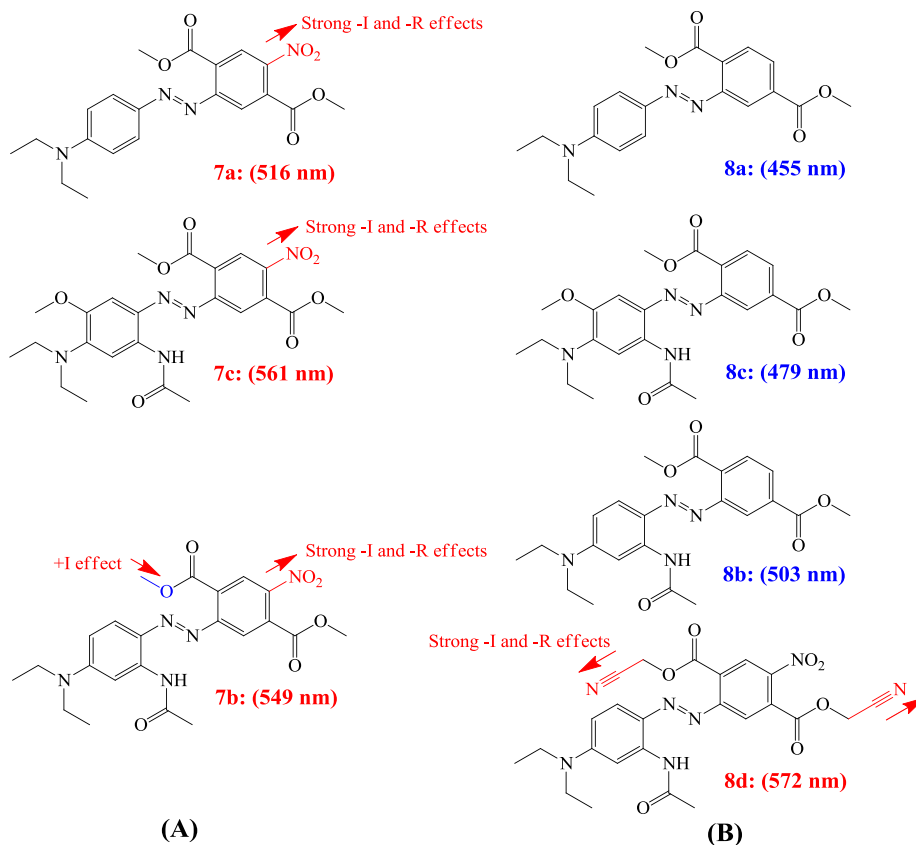


Fig. 2. Correlation of synthesized mono azo disperse dye (A) with an analogous reported dye (B) in DMF.

results showed that these dyes exhibit strong solvatochromic properties. The presence of electron donor unit shows red shift which may be due to the fact that electron favors the intramolecular charge transfer (ICT) effect [7]. Red shifted absorption of **7b** compared to **7a** may be attributed to the planarity associated with the hydrogen bonding between the hydrogen of acetamido and azo nitrogen atom. Such a hydrogen bonding is absent in **7a**.

The absorption spectra of dye **7a** showed red shift with the increase in the solvent polarity. The compound **7a** shows absorption maxima at 492 nm in dichloromethane and 516 nm in DMF. Similarly, dyes **7b** and **7c** show absorption maxima at 522 and 537 nm in

dichloromethane and ethanol and at 549 nm in dichloromethane and 561 nm in DMF respectively (Tables 1–3 and Fig. 3). The dyes **7a**, **7b** and **7c** show a shift of 24, 27 and 24 nm respectively, shift in the absorption maxima in different solvents of varying polarities (Fig. 4). The comparison of **7a** (516 nm) with the compounds **7b** and **7c**, the compounds **7b** and **7c** show a red shifted absorption 549 nm for **7b** and 561 nm for **7c** in DMF respectively. The red shift of CT band of **7b–7c** indicates that acetamido and methoxy as well as acetamido unit present on donor unit maintained planarity and hydrogen bonding effect than unsubstituted *N,N*-diethylaniline unit present in **7a**. This fact is supported by DFT. Push–pull charge transfer mechanism in D– π –A type chromophore **7b** is illustrated in Fig. 5.

Table 1

Observed UV–visible absorption and computed absorption spectra at B3LYP/6-31G(d) for dyes **7a** in different solvent.

Medium	Experimental		Computed (TD-DFT)			%D ^d
	λ_{\max}^a (nm)	ϵ Molar absorptivity (dm^3 $\text{mol}^{-1} \text{cm}^{-1}$)	Vertical ^b excitation (nm)	f^c	Orbital contribution band gap (eV)	
THF	510	91,660	534	0.640	H \rightarrow L (56%)	4.7
DCM	492	71,829	535	0.777	H \rightarrow L (67%)	8.7
Acetone	510	76,383	537	0.852	H \rightarrow L (79%)	5.3
Ethanol	504	78,205	538	0.870	H \rightarrow L (85%)	6.7
Methanol	498	74,768	538	0.850	H \rightarrow L (82%)	8.0
Acetonitrile	498	67,979	538	0.873	H \rightarrow L (82%)	8.0
DMF	516	91,949	542	0.940	H \rightarrow L (90%)	5.0
DMSO	516	82,759	542	0.937	H \rightarrow L (90%)	5.0

^a Experimental absorption wavelength.

^b Computed absorption wavelength.

^c Oscillator strength.

^d (%D) Deviation between experimental absorption and vertical excitation computed by DFT.

3.2. Optimized geometries of dyes **7a**, **7b** and **7c**

Ground state geometries of the dyes were optimized at B3LYP/6-31G(d) levels for dyes **7a–7c**. A small twisting was observed between C₂–C₁–C₂₈–C₂₉ (**7a**: 27.20, **7b**: 20.60 and **7c**: 21.51) in DMF (Figs. S1–S5). The variation of twist dihedral angle of **7a**, **7b** and **7c** from non-polar to polar solvents are 0.477, 0.408 and 0.143 respectively. It is concluded that resulting optimized geometry of dyes has little small twist dihedral angle in polar than non-polar solvent (Table 4). Optimized bond lengths of the synthesized dyes **7a–7c** in DMF are tabulated in (Table S1). The N=N bond lengths are 1.279, 1.291, 1.294 for dyes **7a–7c**. The N–H bond lengths are 1.024, 1.025 for **7b–7c**, the increased N–H bond length is due to the hydrogen bonding between N₂₇ and H₄₀ atom [8]. While the hydrogen bonding between N₂₇···H₄₀ for **7b–7c** in DMF chromophores are 1.880 and 1.875 at B3LYP/6-31G(d) levels of calculations respectively. From the computational data (Calculated energies (E/

Table 2Observed UV–visible absorption and computed absorption spectra at B3LYP/6-31G(d) for dye **7b** in different solvent.

	Experimental		Computed (TD-DFT)				Computed (TD-DFT)			
	λ_{\max}^a (nm)	ϵ Molar absorptivity ($\text{dm}^3 \text{mol}^{-1} \text{cm}^{-1}$)	Azo		Hydrazone		Azo		Hydrazone	
			Vertical ^b excitation (nm)	f^c	Orbital contribution band gap (eV)	%D ^d	Vertical ^b excitation (nm)	f^c	Orbital contribution band gap (eV)	%D ^d
a	540	30,380	518	1.125	H → L (98%)	4.1	459	1.206	H-1 → L (95%)	15
b	522	26,235	520	1.131	H → L (98%)	0.4	460	1.213	H-1 → L (95%)	12
c	534	27,648	521	1.106	H → L (98%)	2.4	459	1.189	H-1 → L (95%)	14
d	528	27,742	521	1.102	H → L (98%)	1.3	460	1.190	H-1 → L (95%)	13
e	525	27,554	520	1.093	H → L (98%)	1.0	459	1.177	H-1 → L (95%)	13
f	525	22,938	521	1.093	H → L (98%)	0.8	459	1.183	H-1 → L (95%)	13
g	549	23,927	525	0.909	H → L (85%)	4.4	462	1.214	H-1 → L (95%)	16
h	543	26,093	524	0.929	H → L (85%)	3.5	462	1.209	H-1 → L (95%)	15

Where, a = Tetrahydrofuran, b = Dichloromethane, c = Acetone, d = Ethanol, e = Methanol, f = Acetonitrile, g = N,N-Dimethylformamide, h = Dimethyl sulphoxide.

^a Experimental absorption wavelength.^b Computed absorption wavelength.^c Oscillator strength.^d (%D) Deviation between experimental absorption and vertical excitation computed by DFT.

hartree), Gibbs free energies ($\Delta G/\text{hartree}$), Relative energies ($\Delta E/\text{kJ mol}^{-1}$), Electronic vertical excitation spectra (TD-DFT) and Interatomic distance) it is observed that compounds exit in only azo form (Tables S2–S3).

The Mulliken charge distribution in ground state (DMF solvent) on selected atoms of the dyes **7a**, **7b** and **7c** are shown in Table S4. In the ground state, charge on the atom N₂₅ and C₇ was found to be nearly same but atom N₂₇ and N₃₉ observed some changes for azo and hydrazone form of dyes **7b–7c**. The negative charge in azo form is more located on the amide nitrogen N₃₉ compared to the nitrogen N₂₇. The Mulliken charge distribution results suggest that azo form is more stable than hydrazone form of dyes **7b–7c** (see Figs. S6–S10) [22]. Mulliken charge distribution of dyes **7a–7c** is summarized in Table S4 by using Gauss View 5.0 software [23].

3.3. Calculated energies of azo-hydrazone tautomeric forms

To find out stability of azo and azo-hydrazone forms calculated energies ($E/\text{hartree}$), Gibbs free energies ($\Delta G/\text{hartree}$) and relative energies ($\Delta E/\text{kJ mol}^{-1}$) of the chromophores **7b–7c** in their azo and hydrazone tautomeric forms calculated at B3LYP/6-31G(d) level (Table S2–S3). It is clear that the azo form is relatively more stable than the corresponding hydrazone form by 48.00, 47.67 kJ mol^{-1}

level in gas phase. The calculated energies ($E/(\Delta G/\text{hartree})$) and relative energies ($\Delta E/\text{kJ mol}^{-1}$) in different solvents also show that the azo forms are slightly more stable in non-polar solvents as compared to polar solvents [24].

3.4. Electronic vertical excitation spectra (TD-DFT)

Electronic vertical excitations were calculated using TD-B3LYP/6-31G(d) method in gas phase as well as in tetrahydrofuran, dichloromethane, acetone, ethanol, methanol, acetonitrile, n,n-dimethylformamide, dimethyl sulphoxide solvent of different polarities. Computed vertical excitation spectra associated with their oscillator strength (f), orbital contribution and band gap as well as their experimental absorbance spectra of the dyes **7a–7c** are shown in (Tables 1–3). The absorption band at lower energy with higher oscillator strength is due to intramolecular charge transfer (ICT) and is characteristic of donor- π -acceptor push-pull dyes. These ICT bands for all dyes mainly occurred due to the electronic transition from highest occupied molecular orbital (HOMO) to lowest unoccupied molecular orbital (LUMO).

The dye **7a** shows blue shifted absorption in dichloromethane (492 nm) and red shifted absorption in DMF (516 nm). The vertical excitation of the dye **7a** were computed and it shows blue shift absorption in THF (534 nm) and red shift in DMF

Table 3Observed UV–visible absorption and computed absorption spectra at B3LYP/6-31G(d) for dye **7c** in different solvent.

	Experimental		Computed (TD-DFT)				Computed (TD-DFT)			
	λ_{\max}^a (nm)	ϵ Molar absorptivity ($\text{dm}^3 \text{mol}^{-1} \text{cm}^{-1}$)	Azo		Hydrazone		Azo		Hydrazone	
			Vertical ^b excitation (nm)	f^c	Orbital contribution band gap (eV)	%D ^d	Vertical ^b excitation (nm)	f^c	Orbital contribution band gap (eV)	%D ^d
a	540	5862	579	0.850	H → L (95%)	7.2	470	0.710	H-1 → L (67%)	13
b	540	6613	581	0.860	H → L (95%)	7.6	470	0.644	H-1 → L (61%)	13
c	543	5611	582	0.844	H → L (95%)	7.2	483	0.482	H-1 → L (50%)	11
d	537	6012	583	0.846	H → L (95%)	8.6	483	0.517	H-1 → L (54%)	10
e	537	6914	582	0.835	H → L (95%)	8.4	482	0.526	H-1 → L (54%)	10
f	543	6112	583	0.841	H → L (95%)	7.4	482	0.553	H-1 → L (56%)	11
g	561	6764	587	0.874	H → L (95%)	4.6	484	0.638	H-1 → L (65%)	14
h	561	7415	587	0.870	H → L (95%)	4.6	484	0.647	H-1 → L (65%)	14

Where, a = Tetrahydrofuran, b = Dichloromethane, c = Acetone, d = Ethanol, e = Methanol, f = Acetonitrile, g = N,N-Dimethylformamide, h = Dimethyl sulphoxide.

^a Experimental absorption wavelength.^b Computed absorption wavelength.^c Oscillator strength.^d (%D) Deviation between experimental absorption and vertical excitation computed by DFT.

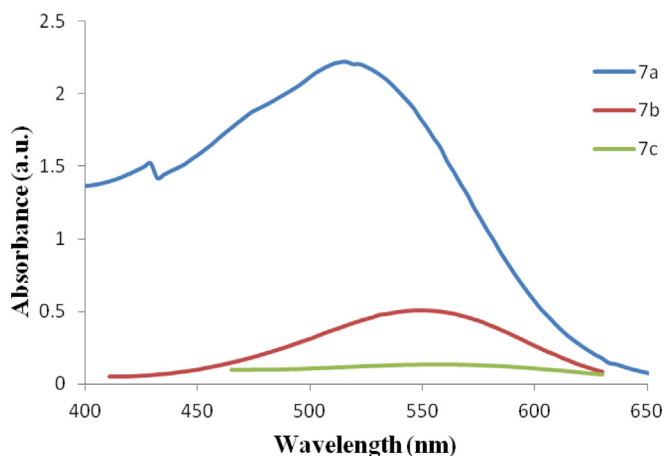


Fig. 3. Absorption spectra of dyes **7a**, **7b** and **7c** (in DMF).

(542 nm). Similar, solvatochromic results were obtained for dyes **7b** and **7c**. The chromophores **7b** and **7c** experimental (vertical excitation) absorption show blue shift absorption in dichloromethane 522 nm, (THF 518 nm) and methanol 537 nm (THF 579 nm), while red shift absorption in DMF at 549 nm (525 nm) and 561 nm (587 nm) respectively. The vertical excitations of azo form having less percent of deviation with experimental data as compared to hydrazone form summarized in Tables 1–3. The largest (minimum) percentage deviation between the experimental absorption maxima and computed vertical excitation is 8.7 nm in dichloromethane (4.7 nm in THF), 4.4 nm in

DMF (0.4 nm dichloromethane) and 8.6 nm ethanol (4.6 nm DMF) for dyes **7a**, **7b** and **7c** respectively.

3.5. Frontier molecular orbitals

The different frontier molecular orbitals were studied to understand the electronic transition and charge delocalization within these push–pull chromophores. The comparative increase and decrease in the energy of the occupied (HOMO's) and virtual orbitals (LUMO's) gives a qualitative idea of the excitation properties and the ability of hole or electron injection [25]. First allowed and the strongest electron transitions with largest oscillator strength usually correspond almost exclusively to the transfer of an electron from HOMO → LUMO (Tables S5–S7) and shows the energies of different molecular orbitals involved in the electronic transitions of these push–pull dyes in different solvents. It was observed that electronic transition in each case included HOMO → LUMO transition. In the case of all synthesized azo disperse dye **7a–7c**, the energy gap of HOMO and LUMO orbitals were decreased as the solvent polarity was increased (Fig. 6, and Figs. S11–S12, Tables S5–S7). The LUMO energy level of the compound **7a–7c** are -3.04 , -3.07 , and -3.07 eV in DMF remained same, and it may be due to the very similar reduction potential (Fig. 7) of the dyes **7a–7c**. This is understandable because of the reduction site, assuming the carbonyl of ester and nitro has the same chemical structure in three molecules [26].

Molecular orbital diagrams of the dyes **7a–7c** are shown in (Fig. 7), from the pictorial diagram, it is clear that the electron densities in the HOMOs of all these three dyes were largely located on donor N,N-diethylaniline moiety, and electron densities on the

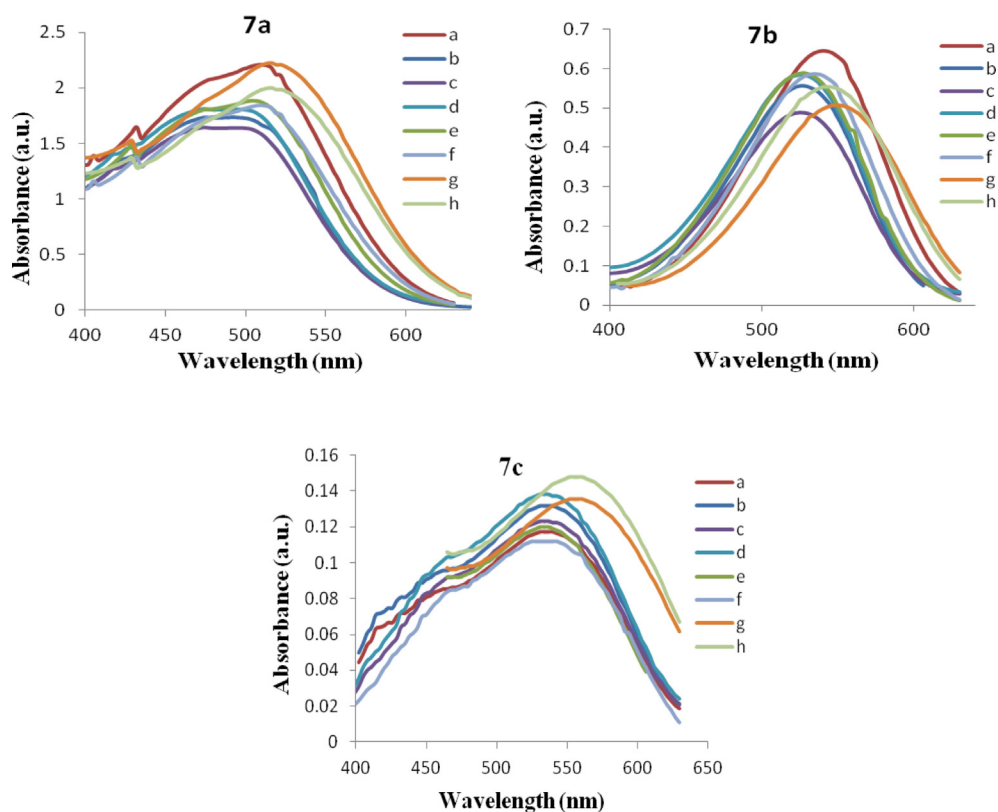


Fig. 4. Absorption spectra of dyes **7a**, **7b** and **7c** in different solvent. Where, a=Tetrahydrofuran, b=Dichloromethane, c= Acetone, d=Ethanol e=Methanol, f= Acetonitrile, g= N,N-Dimethylformamide, h=Dimethyl sulphoxide.

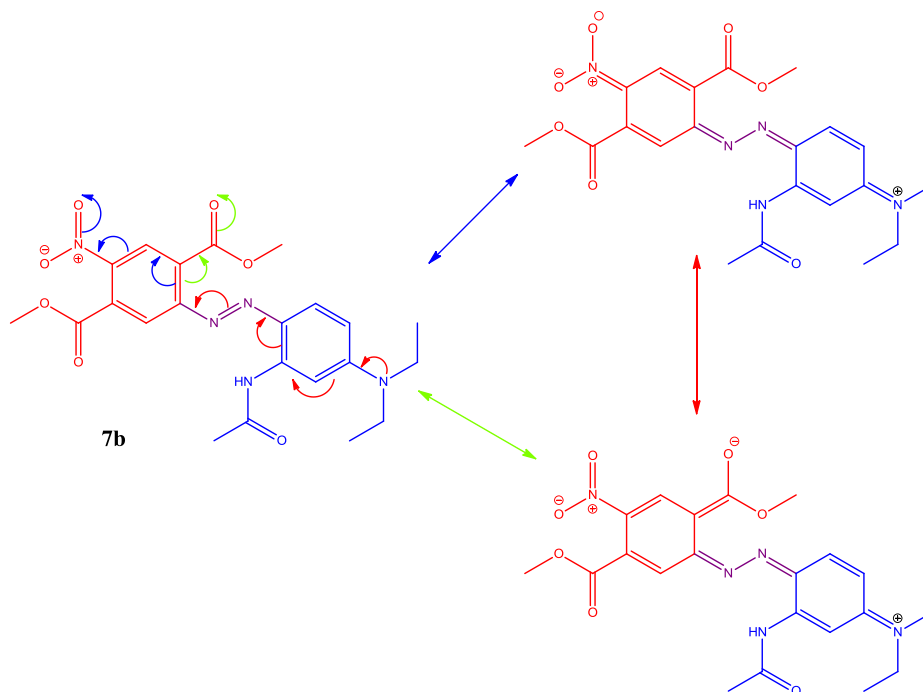


Fig. 5. Charge transfer mechanism in push-pull chromophore of D- π -A (dye **7b**).

LUMOs were found localized on acceptor through azo π -bridge. The excitation from HOMO to LUMO mostly consists of charge transfer from donor *N,N*-diethylaniline moiety to the acceptor end. The energy gap of HOMO \rightarrow LUMO explains the charge transfer interactions within the dye.

4. General procedure of dyeing [27,28]

Disperse dyeing of polyester and nylon fabric was carried out using high temperature high pressure method in Rossari Labtech Flexi Dyer dyeing machine with a material to liquor ratio of 1:20. 2% Dye was used for fabric dyeing (calculated on weight of the fabric). All synthesized azo disperse dyes are having very less solubility in water. Firstly dye was dissolved in 5 ml *N,N*-dimethylformamide and diluted with 15 ml buffered solution of pH 5 made by using sodium acetate and acetic acid in water. Fine dispersion of the dye in water was obtained after ultrasonication for 15 min. Metamol was used as a dispersant. Polyester fabric and nylon were dyed using the above solution. Dyeing was commenced at room temperature. The dye bath temperature was raised at a rate of $3\text{ }^{\circ}\text{C min}^{-1}$ – $130\text{ }^{\circ}\text{C}$ and $80\text{ }^{\circ}\text{C}$ respectively, maintained at this temperature for 60 min, and rapidly cooled to $50\text{ }^{\circ}\text{C}$ as depicted in Fig. 8. The dyed fabrics were rinsed under cold water and then reduction cleared in an aqueous solution

Table 4
Dihedral angle between C_2 – C_1 – C_{28} – C_{29} of dyes **7a**, **7b** and **7c** in different solvent.

Solvents	7a	7b	7c
	Dihedral angle	Dihedral angle	Dihedral angle
THF	27.64	21.02	21.64
DCM	27.56	20.92	21.63
Acetone	27.33	20.66	21.57
Ethanol	27.28	20.63	21.55
Methanol	27.23	20.61	21.52
Acetonitrile	27.21	20.61	21.52
DMF	27.20	20.61	21.51
DMSO	27.16	20.61	21.50

of 1 g L^{-1} sodium hydrosulfite and 1 g L^{-1} sodium hydroxide using 1:50 liquor to goods ratio at $80\text{ }^{\circ}\text{C}$ for 30 min. The treated fabrics were rinsed by cold water and allowed to dry in the open air.

5. Fastness properties

Washing, sublimation, light fastness and color match properties were done by using standard procedure [27,28].

5.1. Fastness to washing

Wash fastness property depends upon the solubility of dye in water, size of dye molecules, charge present on the dye and which type of linkage present in dye molecule and fabrics. A sample of dyed fabric was washed in solution (3 g L^{-1} Na_2CO_3 , 1 g L^{-1} NaOH) at $60\text{ }^{\circ}\text{C}$ for 30 min. The change in tone of washed fabrics was assessed by the international standard scale IS: 765-1979 (1 for poor and 5 for excellent) given in (Table 5).

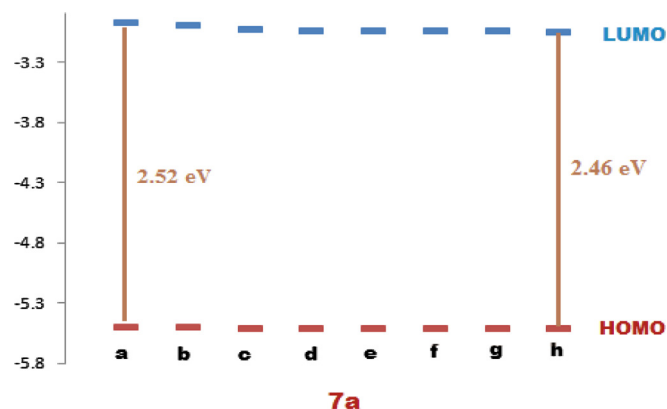


Fig. 6. Energy gap between HOMO \rightarrow LUMO of the dye **7a** in different solvent.

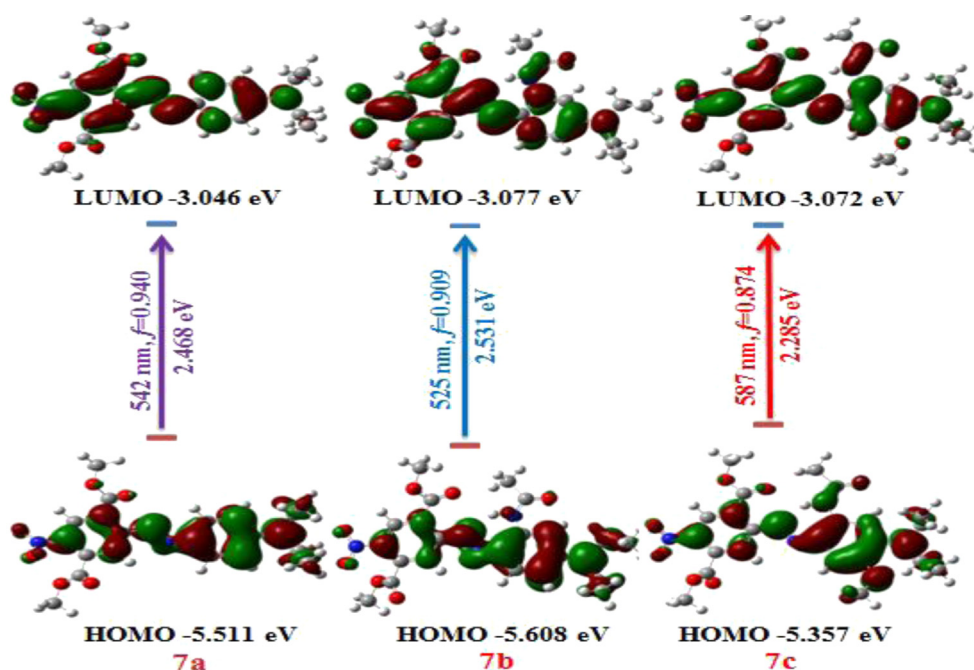


Fig. 7. Frontier molecular orbitals of dyes **7a**, **7b** and **7c** in the ground state.

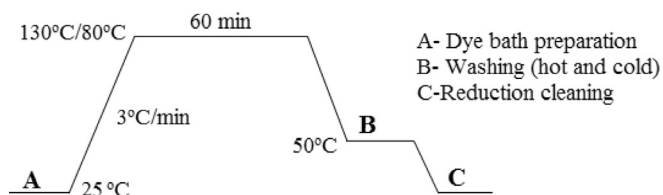


Fig. 8. Dyeing profile of polyester/Nylon used in this study.

5.2. Fastness to sublimation

Sublimation fastness is the most significant requirement of dyed fabrics, as migration of dye molecules and wet fastness of azo disperse dyes on dyed fabrics are totally depended on heat treatment. Sublimation fastness and staining of **7a–7c** azo disperse dyes on the undyed polyester-cotton and nylon-cotton for polyester and nylon respectively showed poor to moderate ratings because of presence of ester moiety. The ratings were done by the international geometric gray scale.

5.3. Fastness to light

Light fastness is the degree to which a dye resists fading due to light exposure. All synthesized dyes have quite susceptible to light

damage which fully depends on molecular structure. According to the AATCC test method all dye showed good light fastness on both polyester and nylon fabrics.

6. Color assessment

The colorimetric parameters of the dyed polyester and nylon fabrics using the synthesized azo disperse dyes **7a–7c** were recorded on a reflectance spectrophotometer CE-7000A Gretag-Macbeth. CIE 1976 Color Space method used to evaluate color values of the synthesized azo disperse dyes **7a–7c** on both the polyester and nylon fabrics in terms of L^* , a^* and b^* (Table 6). All the dyes have good affinity towards the polyester fabrics at high temperature and gave red shades on polyester fabrics. The values of color coordinates suggested that the color hue of dyes **7a** of polyester and nylon shifted towards the redder direction on the red-green axis as well as towards the yellowish direction on yellow-blue axis as positive values of a^* and b^* respectively. While color hue of dyes **7b** and **7c** of polyester and nylon shifted towards bluish direction on the yellow-blue axis as negative values of b^* (Table 6). Color strength of all dyes applied on polyester and nylon fabrics are expressed as K/S values which are dependent on the type of substituent present on the aromatic ring. K/S values of these dyes showed polyester have eight to ten time good dyeing properties as compared to nylon.

Table 5
Fastness properties of azo disperse dyes **7a–7c** on polyester and nylon fabrics.

Fabrics	Dye no.	Light fastness (1–8)	Wash fastness (1–5)	Staining on fabric after washing (1–5)		Sublimation fastness (1–5)	Staining on fabric after sublimation (1–5)	
				Polyester/Nylon	Cotton		Polyester/Nylon	Cotton
Polyester	7a	7	5	5	5	3	2	2
	7b	7	5	5	5	3	1–2	1–2
	7c	6	4–5	4–5	5	4	4	3–4
Nylon	7a	6	4–5	4–5	4–5	4–5	4	3–4
	7b	7	4–5	5	4	4	3–4	3
	7c	6	4	4	4–5	4	3–4	3

Light fastness: (Grading: 1- poor, 2- slight, 3- moderate, 4- fair, 5- good, 6- very good, 7- excellent).

Wash fastness: (Grading: 1- poor, 2- fair, 3- good, 4- very good, 5- excellent).

Table 6Color values of terephthalate azo disperse dyes **7a–7c** on polyester and nylon fabrics.

Fabrics	Dye no.	L*	a*	b*	c*	Ho	K/S
Polyester	7a	57.65	29.90	11.88	32.18	21.65	14.72
	7b	56.62	26.99	−13.92	30.37	332.73	16.46
	7c	72.70	8.62	−7.02	11.11	320.87	4.14
Nylon	7a	59.52	29	4.68	29.38	9.17	1.97
	7b	56.32	13.28	−13.85	19.19	313.8	1.61
	7c	72.20	8.20	−6.98	10.77	319.62	0.44

7. Conclusion

In this paper, we report the synthesis of three D- π -A mono azo dyes containing *N,N*-diethylaniline as the electron donor and the electron withdrawing nitro/carbomethoxy group. These synthesized dyes were confirmed by FT-IR, ^1H NMR, ^{13}C NMR, Mass and HRMS spectral analysis. All the disperse azo dyes show very good fastness properties except sublimation which can be attributed to the presence of the ester group. The vertical excitation spectra were computed at B3LYP/6-31G(d) level and compared with the experimental values. The results clearly indicate the dyes **7b** and **7c** only exist in the azo. Frontier molecular orbital diagram shows electron density of chromophores is slightly more concentrated on the donor moiety in the ground state HOMO and also the observed absorbance at longer wavelength is due to the HOMO \rightarrow LUMO with high oscillator strength.

Acknowledgments

The authors are greatly thankful to TIFR, SAIF-I.I.T. Mumbai for recording the ^1H NMR and Mass spectra. One of the authors Mininath S. Deshmukh is grateful to CSIR for financial support.

Appendix A. Supplementary data

Supplementary data related to this article can be found at <http://dx.doi.org/10.1016/j.dyepig.2013.10.035>.

References

- (a) Karapinar E, Aksu I. An investigation of fastness properties of textile materials colored with azo dyes. *J Textiles Engineer* 2013;20:17–24; (b) Koh J, Greaves AJ. Synthesis and application of an alkali-clearable azo disperse dye containing a fluorosulfonyl group and analysis of its alkali-hydrolysis kinetics. *Dyes Pigm* 2001;50:117–26.
- (a) Raghavendra KR, Kumar AK. Synthesis of some novel azo dyes and their dyeing, redox and antifungal properties. *Int J Pharmaceut Chem Biol Sci* 2013;5:1756–60; (b) Vijayaraghavan R, Vedaraman N, Surianarayanan M, MacFarlane DR. Extraction and recovery of azo dyes into an ionic liquid. *Talanta* 2006;69(5): 1059–62.
- Machida S, Araki M, Matsuo K. Studies of the water-soluble polymers. XVI. Azo dyes of poly-N-vinylimidazole. *J App Poly Sci* 1968;12(2):325–32.
- Nunes GE, Sehnem AL, Bechtold IH. Self-assembled azo-dye film as an efficient liquid crystal aligning layer. *Liquid Crystals* 2012;39:205–10.
- Nejati K, Rezvani Z, Seyedahmadian M. The synthesis, characterization, thermal and optical properties of copper, nickel, and vanadyl complexes derived from azo dyes. *Dyes Pigm* 2009;83:304–11.
- (a) Jinhee P, Daqiang Y, Khanh TP, Jian-Rong L, Andrey Y, Hong-Cai Z. Reversible alteration of CO_2 adsorption upon photochemical or thermal treatment in a metal–organic framework. *J Am Chem Soc* 2012;134:99–102; (b) Dou YS, Hu Y, Yuan SA, Wu WF, Tang H. Detailed mechanism of *trans*–*cis* photoisomerization of azobenzene studied by semiclassical dynamics simulation. *Mol Phys* 2009;107:181–90.
- (a) Li YW, Guo Q, Li ZF, Pei JN, Tian WJ. Solution processable D-A small molecules for bulk-heterojunction solar cells. *Energy Environ Sci* 2010;3: 1427–36; (b) Walker B, Kim C, Nguyen TQ. Small molecule solution-processed bulk heterojunction solar cells. *Chem Mater* 2011;23:470–82.
- Krzysztof W. Spectral properties of disperse dyes, derivatives of *n*-methyl-naphthalimidoazobenzene. *Dyes Pigm* 1990;12:273–86.
- Sokolovska-Gajda J, Kraska J. Synthesis and properties of monoazo disperse dyes derived from the ethyl ester of *n*-benzyl-*n*-phenyl- β -alanine. *Dyes Pigm* 1989;10:285–94.
- Viscardia G, Quagliottoa P, Baroloa C, Diulgheroffa N, Caputo G, Barnia E. Chemichromic azodye from 2,4-dinitrobenzenediazonium *o*-benzenedisulfonimide and *g*-acid for monitoring blood parameters: structural study and synthesis optimisation. *Dyes Pigm* 2002;54:131–40.
- Cristina C, Paul R. Synthesis and optical storage properties of a novel poly-methacrylate with benzothiazole azo chromophore in the side chain. *J Mater Chem* 2004;14:2909–16.
- Frisch MJ, Trucks GW, Schlegel HB, Scuseria GE, Robb MA, Cheeseman JR, et al. Gaussian 09, revision C.01. Wallingford CT: Gaussian, Inc; 2010.
- Treutler O, Ahlrichs R. Efficient molecular numerical integration schemes. *J Chem Phys* 1995;102:346–54.
- Becke AD. A new mixing of Hartree–Fock and local density-functional theories. *J Chem Phys* 1993;98:1372–7.
- Lee C, Yang W, Parr RG. Development of the Colle–Salvetti correlation-energy formula into a functional of the electron density. *Phys Rev B* 1988;37: 785–9.
- (a) Hehre WJ, Radom L, Schleyer PvR, Pople JA. Ab initio molecular orbital theory. New York: Wiley; 1986; (b) Bauernschmitt R, Ahlrichs R. Treatment of electronic excitations within the adiabatic approximation of time dependent density functional theory. *Chem Phys Lett* 1996;256:454–64; (c) Furche F, Rappaport D. Density functional theory for excited states: equilibrium structure and electronic spectra. In: Olivucci M, editor. *Computational photochemistry*. Amsterdam: Elsevier; 2005. p. 16 [Chapter 3].
- Tomasi J, Mennucci B, Cammi R. Quantum mechanical continuum solvation models. *Chem Rev* 2005;105:2999–3094.
- Heldmann C, Schulze M, Wegner G. Rigid-rod-like main chain polymers with rigidly attached chromophores. A novel structural concept for electrooptical materials. 1. Synthesis and characterization. *Macromolecules* 1996;29:4686–96.
- Yuanjing C, Guodong Q, Lujian C, Zhiyu W, Minquan W. Synthesis and nonlinear optical properties of a series of azo chromophore functionalized alkoxy silanes. *Dyes Pigm* 2008;77:217–22.
- Deulgaonkar DS. Institute of Chemical Technology Mumbai. PhD-Tech Thesis; 2008.
- DYSTAR TEXTILFARBEN GMBH & CO [DE], Disperse azo dyestuffs. WO patents 2007;1, 018,28A2.
- Lien V, Karen H, Veronique V, Karen D. The influence of a polyamide matrix on the halochromic behaviour of the pH-sensitive azo dye nitrazine yellow. *Dyes Pigm* 2012;94:443–51.
- Dennington R, Keith T, Millam J. Gaussview version 5.0. Shawnee Mission KS: Semiche Inc; 2009.
- Umape PG, Patil VS, Padalkar VS, Phatangare KR, Gupta VD, Tathe AB, et al. Synthesis and characterisation of novel yellow azo dyes from 2-Morpholin-4-yl-1,3-thiazol-4(5H)-one and study of their azo-hydrazone tautomerism. *Dyes Pigm* 2013;99:291–8.
- Gupta VD, Tathe AB, Padalkar VS, Umape PG, Sekar N. Red emitting solid state fluorescent triphenylamine dyes: synthesis, photo-physical property and DFT study. *Dyes Pigm* 2013;97:429–39.
- Chen CT, Chiang CL, Lin YC, Chan LH, Huang CH, Chen CT. Ortho-substituent effect on fluorescence and electroluminescence of arylamino-substituted coumarin and stilbene. *Org Lett* 2003;5:1261–4.
- Satam MA, Raut RK, Sekar N. Fluorescent azo disperse dyes from 3-(1,3-benzothiazol-2-yl)naphthalen-2-ol and comparison with 2-naphthol analogs. *Dyes Pigm* 2013;96:92–103.
- Shukla SR, Mathur MR. Low temperature ultrasonic dyeing of silk. *J Soc Dyers Colorists* 1995;111:342–5.